Solar Physics (2005) 230: 111–127

THE TOTAL IRRADIANCE MONITOR (TIM): INSTRUMENT CALIBRATION

GREG KOPP, KARL HEUERMAN and GEORGE LAWRENCE
Laboratory for Atmospheric and Space Physics, University of Colorado, Boulder, CO 80309, U.S.A.
(e-mail: kopp@lasp.colorado.edu)

(Received 7 February 2005; accepted 13 May 2005)

Abstract. The calibrations of the SORCE Total Irradiance Monitor (TIM) are detailed and compared against the designed uncertainty budget. Several primary calibrations were accomplished in the laboratory before launch, including the aperture area, applied radiometer power, and radiometer absorption efficiency. Other parameters are calibrated or tracked on orbit, including the electronic servo system gain, the radiometer sensitivity to background thermal emission, and the degradation of radiometer efficiency. The as-designed uncertainty budget is refined with knowledge from the on-orbit performance.

1. Introduction

The Total Irradiance Monitor (TIM) is an ambient temperature electrical substitution solar radiometer designed to achieve 100 parts per million (ppm) combined standard uncertainty in total solar irradiance (TSI). The TIM contains four electrical substitution radiometers (ESRs), which are electrically heated to maintain constant temperature while a shutter modulates sunlight through a precision aperture and into an ESR's absorptive cavity. The modulation in electrical heater power needed to maintain an ESR's temperature as its shutter modulates incident sunlight determines the radiative power absorbed by that ESR's cavity. Phase sensitive detection of this heater power, combined with knowledge of the aperture area over which the sunlight is collected, yields TSI in ground processing.

Meeting the design uncertainties presented by Kopp and Lawrence (2005) requires several precision calibrations of components and subsystems in the TIM. The most fundamental calibrations, such as the aperture area, ESR power applied, and cavity absorptivity are ground calibrations. Other items are directly calibrated on orbit. These include the servo system gain and the instrumental thermal infrared contribution to the measured signal. All calibrations are tracked for changes on orbit, including cavity absorptivity. After ground processing of these on-orbit calibrations or calibration changes, the resulting instrument data are updated to include the latest calibration values, many of which can be applied retroactively.

2. Ground Calibrations

Ground calibrations of spacecraft instruments are generally more accurate than possible in flight, as ground-based precision calibration facilities are not constrained

by mass, power, or vibrations typical of launch environments. Ground calibrations are most appropriate for stable components, enabling transfer of the calibration to the in-flight instrument unchanged by age or launch vibrations.

2.1. Cavity absorptance α is near 0.9998

Cavity reflectance 1-α is measured using laser scans mapping the cavity interiors at six wavelengths spanning the spectral peak of the emitted solar flux. These spatially resolved measurements are supplemented by spatially integrating calibrations at mid-infrared wavelengths to extend the spectral coverage. The effective cavity reflectance is the average of the reflectance measurements at individual wavelengths weighted by the solar energy distribution given by Lean (2000).

A spatial map of cavity reflectance from a two-dimensional laser scan is averaged over the region of the cone illuminated by sunlight to obtain an effective reflectance at that laser wavelength. The solar limb-darkened profile is accounted for when computing these averages, and is a $\sim$0.1 ppm effect. Spatial maps, such as that shown in Figure 1, are acquired at each of six laser wavelengths (457, 532, 633, 830, 1064, and 1523 nm) spanning the primary solar spectrum.

The spatially resolved laser measurements are supplemented by a broad-beam laser calibration at 10.6 microns to extend the reflectance calibrations to the mid-infrared. NIST measurements of select cavities from 2 to 20 microns using an FTIR, described by Hanssen *et al.* (2003), fill in the large spectral gaps between the discrete laser wavelengths, and show that the cavity reflectance varies smoothly with wavelength through the mid-infrared.

A spline fit of the reflectance interpolates between the discrete laser wavelength calibrations. This fit is constrained at long wavelengths by estimating a reflectance at 100 μm that maintains a smoothly decreasing slope so the fitted long wavelength reflectance never exceeds unity, and at short wavelengths by the shortest-wavelength reflectance measurement. Since the Sun emits relatively little power at these far-infrared and ultraviolet wavelengths, the uncertainty in the cavity reflectance from this estimate is low. The reflectance calibrations for the primary TIM cavity are shown in Figure 2.

The effective solar-weighted reflectances for the four TIM cavities are very low, with values of 169, 139, 307, and 360 ppm. Reflectance uncertainties are 14%, including nearly equal estimated measurement uncertainty and statistical portions. These ground-based measurements of absorptance are tracked for relative changes on orbit, as described in Section 3.3.

2.2. Aperture area is corrected for diffraction and thermal variations

The areas A of the diamond-turned aluminum apertures were measured at NIST using the non-contact geometric aperture calibration facility described by Fowler,

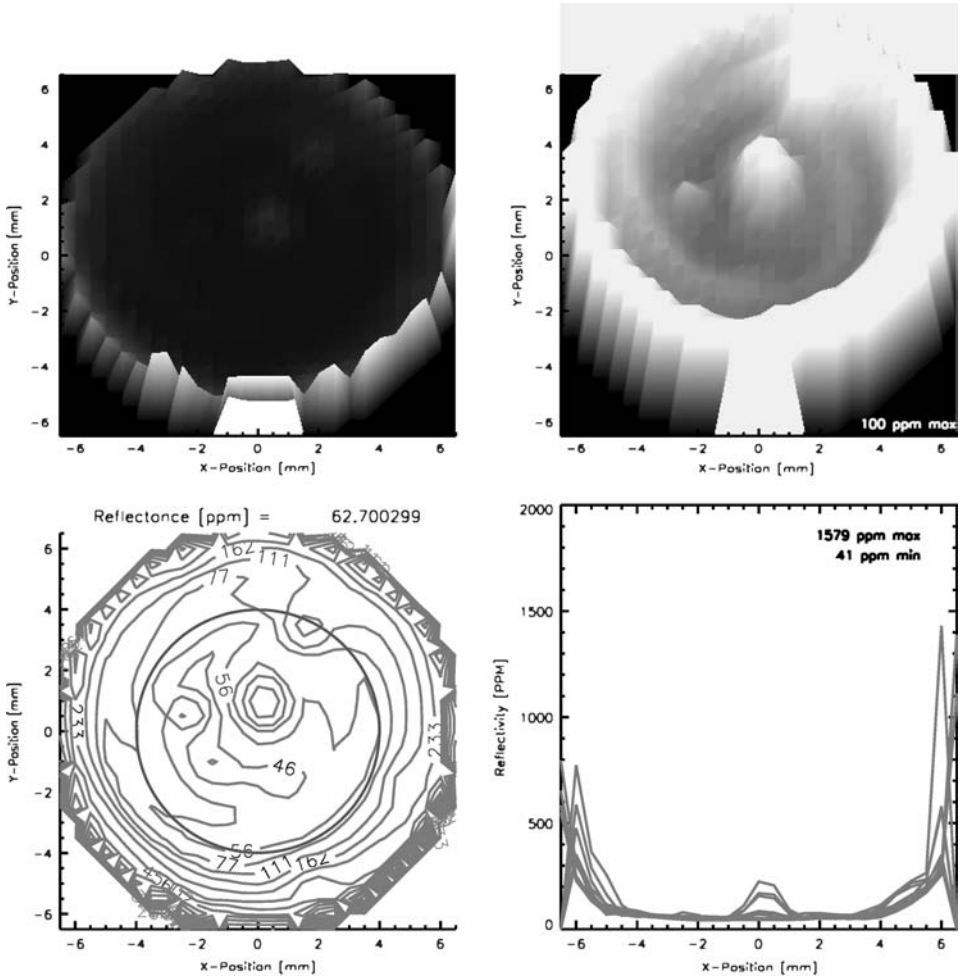

Figure 1. Cavity reflectance spatial map. Maps of the cavity interiors at six wavelengths spanning the solar spectrum peak are used to calibrate the cavity absorptance.

Saunders, and Parr (2000). The four TIM apertures have geometric areas 0.49928, 0.49938, 0.49936, and 0.49926 cm^2 with relative standard uncertainties of 25 ppm. This aperture area is corrected for temperature changes, diffraction, and bulk modulus expansion to the space environment.

Because of the precision with which NIST can measure geometric aperture areas, the dominant TIM aperture area uncertainty is the diffraction correction. This correction is proportional to the energy-weighted average wavelength $\langle\lambda\rangle$ of the solar spectrum and corresponds to a relative TIM diffraction correction of 430 ppm using $\langle\lambda\rangle = 947$ nm, based on measured solar spectra reported by Lean (2000). Shirley (1998, 2000) of NIST advises including 10% (43 ppm) of the diffraction correction as uncertainty.

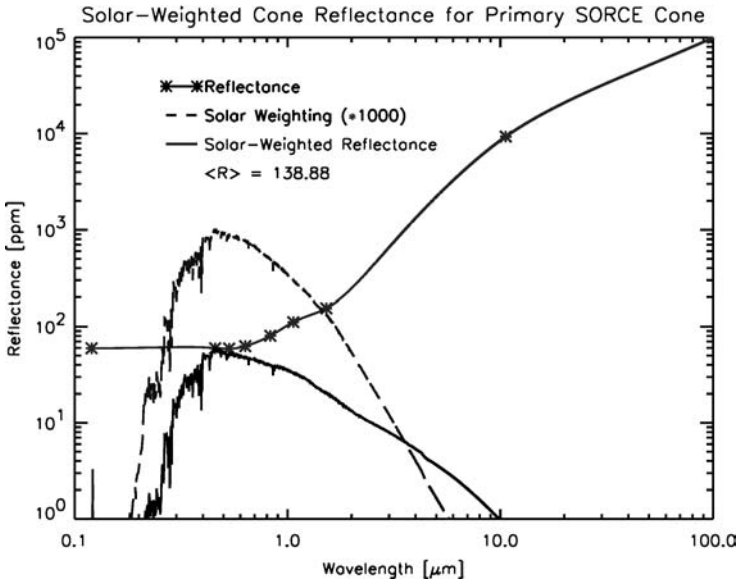

Figure 2. Cavity reflectance spatial calibrations. The cavity reflectance, smoothly fitted between calibrations at discrete laser (*asterisks*), increases with wavelength in the infrared. Cavity reflectance is weighted by the normalized solar spectral irradiance (*dashed line*), giving a relative solar-weighted cavity reflectance (*solid line*); this solar weighting gives the average cavity reflectance used to correct for sunlight not absorbed by the cavity.

We also include corrections for measurements of scattering and reflections from imperfect edges ($\sim$40 ppm) and assembly tolerances on alignments that can affect the amount of diffracted light absorbed. Ground-based measurements of witness aperture areas provide a 2nd order coefficient of thermal expansion appropriate for the flight apertures' aluminum. A platinum resistive thermal device (RTD) provides the flight apertures' temperature used in thermal corrections to the area, which are known to about 12 ppm. Pressure changes between ground calibrations and flight operations increase the flight aperture area by <1 ppm and are corrected. These corrections yield a net uncertainty in aperture area of 55 ppm, as summarized in Table II.

2.3. STANDARD WATT COMES FROM STABLE VOLTAGE AND RESISTANCE REFERENCES

Changes in the electrical heater power applied to the ESRs directly compensate variations of the absorbed radiant power. This electrical power is purely resistive, and is produced by pulse width modulating a voltage standard reference through a standard reference resistor embedded in each ESR. There is no on-orbit monitor of these voltage or resistance references, as no low-mass, space-certified meter with

10^{-6} absolute accuracy is available. Instead, the TIM relies on stable voltage and resistance references that are calibrated and characterized prior to launch. Changes on orbit may be tracked by comparing simultaneous TSI measurements with two ESRs, which have different heater resistors and use different voltage references.

The standard watt relies on a 7.1 VDC reference voltage from temperature-stabilized Linear Technology LTZ1000 Zener diodes applied across resistive windings of encapsulated wire, and on pre-flight ground calibrations using an 8.5-digit HP3458A meter under temperature-controlled conditions. Both the standard voltage and the standard resistors were monitored and found stable throughout instrument assembly, environmental testing, and spacecraft integration and test, with the final calibrations being 3 months prior to launch.

Pre-flight calibrations of the two voltage references give

$$V_1 = 7.166434\,(1 - 0.201404 \times 10^{-6}\,T) \tag{1}$$

$$V_2 = 7.120490\,(1 - 0.112085 \times 10^{-6}\,T) \tag{2}$$

for temperature T in degrees Celsius. These temperature dependences are fairly linear across a 50 °C temperature range, as shown in Figure 3. Pre-flight measurements of the flight standard voltages have been stable to <1 ppm in spite of six qualification temperature cycles from -35 to $+50$ °C. Over 3 years of continual operation, five laboratory copies of the standard voltage circuits have changed in relative voltage by -0.9 ± 0.7 ppm/year (see Figure 4), consistent with the previous

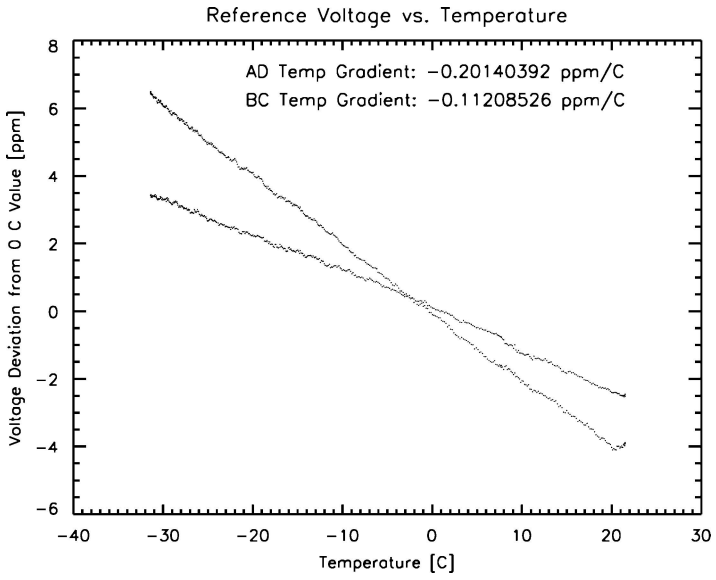

Figure 3. Temperature dependence of standard voltage. The temperature dependence of the LTZ1000 voltage references used in the TIM is linear from -30 to $+20$ °C.

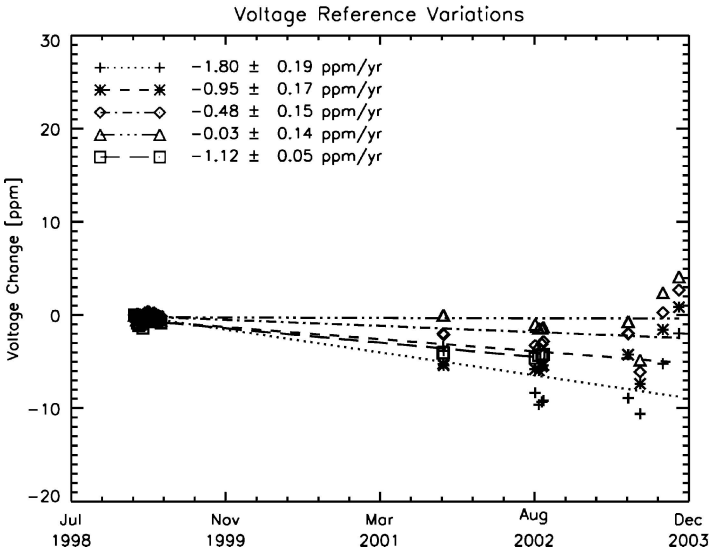

Figure 4. Witness voltage unit stability. Several ground-based LTZ1000 voltage references change by only 1 ppm/year.

studies (Spreadbury, 1991). The flight calibrations of the TIM voltage references are updated for systematic behavior of these five plus eight additional units.

The effective heater resistances for the four ESRs are 543.9689, 538.4464, 546.3407, and 537.9084 Ω at the cavity's operating temperature of 30.8 °C (see Figure 5). Temperature corrections based on four different instrument temperatures are applied to the heater wire and the low-resistance copper electrical leads. Measured temperature coefficients of the MWS heater wire itself are in the range 8–11 ppm/°C, close to the specifications for the 39-MWS-800-HML wire. Qualification temperature cycling of the resistor references has changed their relative resistances less than 3 ppm.

2.4. Power non-linearity is based on ground calibrations of nearly identical flight-like units

While most calibrations met the design uncertainty budget, the flight TIM had an unanticipated non-linear response with varying pulse width in the power applied to the ESRs. This non-linearity is due to the changes in the applied pulse width rise and fall times with varying duty cycle. The effect was only noticed after launch, and is corrected based on the measurements of two ground-based but flight-like TIM instruments, and is consistent with special on-orbit tests with the flight unit.

Power non-linearities measured in the eight ESRs from the two ground-based TIM units are similar but not identical, as shown in Figure 6. Variations between the four ESRs within an individual instrument are smaller than those in different units.

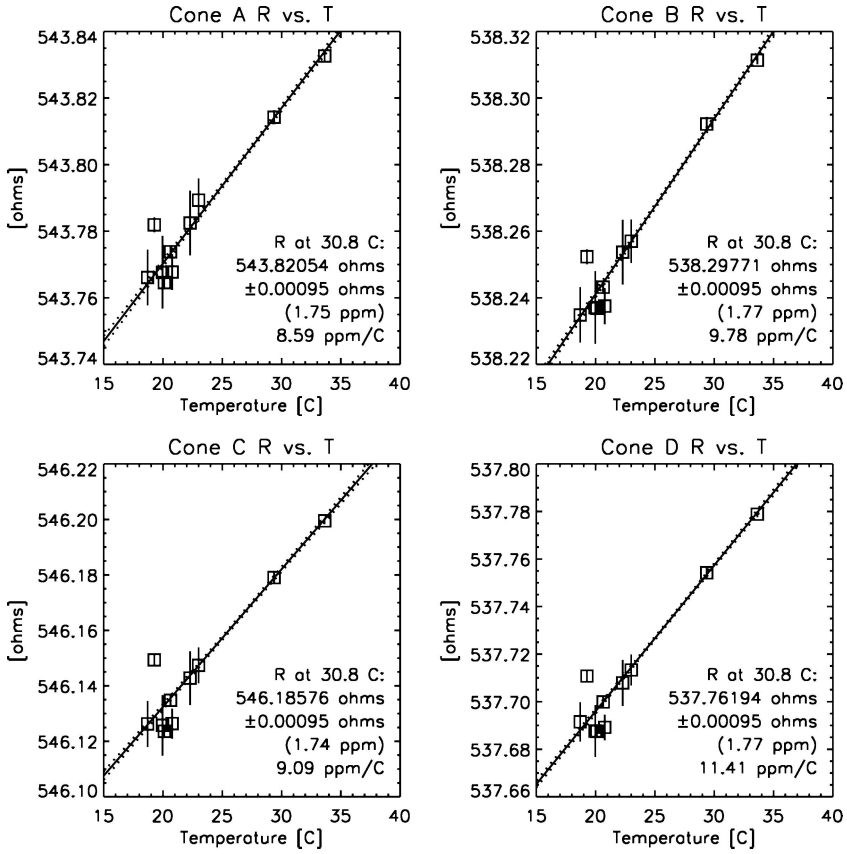

Figure 5. ESR heater resistance calibrations. The effective heater resistance is derived from ground-based calibrations at different temperatures. The contributions from low-resistance leads is removed to determine the effective ESR heater resistance.

The variations between these instruments or between their individual ESRs help determine the uncertainty by which we can expect a ground-based non-linearity determination to correctly apply to the flight unit. The TIM is operated at upper (shutter closed) power levels that are generally below the non-linear region at high duty cycles in the curve in Figure 6; however, the lower (shutter open) power levels used are affected by the non-linear region at low duty cycles, so the knowledge of this non-linearity is important.

Two flight tests help refine these ground-based non-linearity corrections for the flight unit. In the first test, simultaneous solar irradiance observations were made over the course of a day using both the primary and secondary ESRs. While the secondary ESR remained at a nominal power level to track small changes in the Sun's output power, the primary ESR was scanned from the lower limit of its power range to the upper limit. The characteristic non-linearity corrections shown

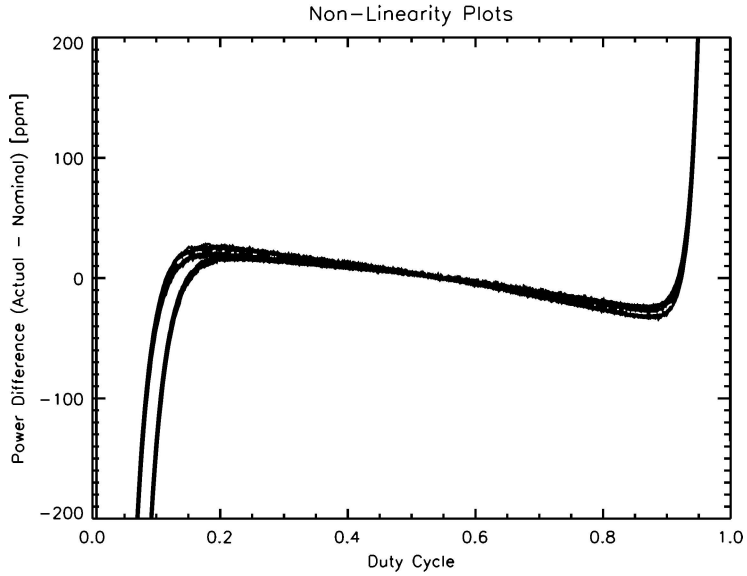

Figure 6. Measured non-linearity corrections. The measured non-linearity of two ground-based TIM units (four ESRs each) is plotted for various duty cycles of the pulse width modulated ESR power. The measurements have been offset to overlap at a 50% duty cycle for this plot. Such vertical offsets do not affect the TIM TSI measurement, as it is due to the difference in power between the shutter closed (high applied power) and open (low duty cycle) states.

in Figure 6 were adjusted very slightly to maintain a nearly constant difference in measured TSI between the two ESRs, meaning that the primary ESR's non-linearity is corrected. The second test comes from intermittent simultaneous observations of the Sun over the course of a year as its measured irradiance varies by $\pm 3.3\%$ due to changes in the Earth–Sun distance. If there are no non-linearities in the applied ESR power, the difference between the two ESRs due to solar distance variations would be zero. The non-linearity corrections shown in Figure 7 include small adjustments to the calibration measurements in Figure 6 that make the flight ESR results consistent with the expected responses for both of these on-orbit tests.

With these linearity adjustments from two ground-based TIM instruments and the on-orbit tests with the flight instrument, we estimate the uncertainty attributable to the flight unit's linearity to have a systematic uncertainty of $\sim$150 ppm and a measurement uncertainty as shown in Figure 7 that can be as high as $\sim$110 ppm. This net uncertainty of $\sim$186 ppm dominates the instrument's uncertainty budget.

2.5. SHUTTER WAVEFORM HAS <1 PPM EFFECT ON IN-PHASE SIGNAL

The shutter moves between a transmission of unity when open, and a transmission <3 ppm when closed. Shutter operation times are 10 ms. For the TIM's 100-s shutter

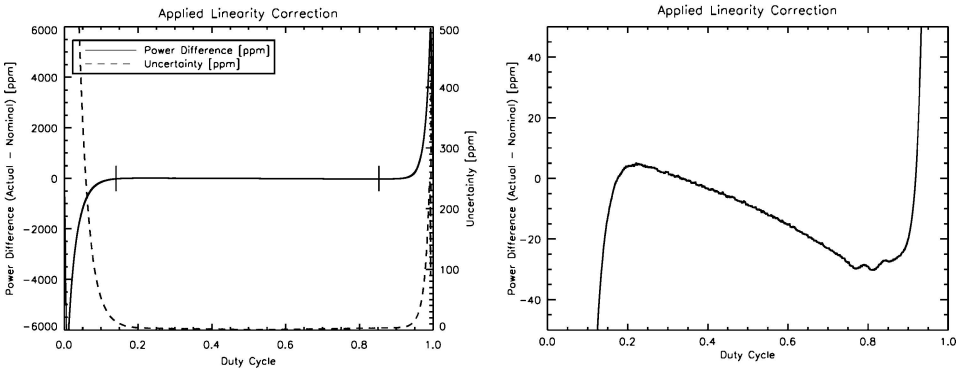

Figure 7. Applied non-linearity correction. The non-linearity of the flight unit is corrected by the plotted amount for various duty cycles of the pulse width modulated ESR power. The *plot on the left* includes vertical markings indicating the nominal power levels used by the primary TIM ESR. This plot also shows the uncertainty in the linearity correction (*right axis*), as estimated from the variations in the linearity measurements plotted in Figure 6. The *plot on the right* is an expanded view of the linearity correction.

period, these shutter operation times produce a relative correction <1 ppm in the phase sensitive analysis of the data. This effect, though small, is accounted for in data processing.

2.6. Pointing sensitivity estimated to be low

A pre-launch field of view (FOV) analysis, based on cavity reflectance maps and variations in the cavity region illuminated as pointing changes, shows <100 ppm relative response up to and past 10 arcmin off-axis. This pointing sensitivity is at least a 2nd order effect, so for the worst case 2 arcmin SORCE pointing errors, no significant TIM pointing effect is expected.

2.7. Equivalence

The equivalence ratio $\mathbf{Z}_H/\mathbf{Z}_R$ comes largely from model calculations, with generous uncertainties in the model parameters, and differs from unity by 7 ppm with an uncertainty of 22 ppm (based on calculations by Lawrence *et al.*, 2000 and described in detail by Kopp and Lawrence, 2005) at the shutter fundamental frequency. The larger non-equivalence at higher harmonics may be used to further constrain the equivalence models. The uncertainty in the equivalence is low because the TIM's phase-sensitive detection only relies on knowledge of the equivalence at one (the shutter fundamental) frequency, and this is a low frequency where the equivalence is very nearly unity.

3. Flight Calibrations

While on-orbit calibrations of space-borne instruments are limited by the sources, power, and thermal environment of the spacecraft and are frequently not of the precision or reproducibility possible using ground facilities, they do offer the advantage and reassurance of post-launch measurements of the instrument performance in the actual flight environment. On the TIM, flight calibrations are conducted to measure thermal contributions to the instrument signal, determine the in-flight servo system gain, and to track degradation affecting the ESRs' absorptance.

3.1. Measurements of dark space provide the instrument's thermal background (dark correction)

The instrument's thermal-background ("dark") signal is measured by observing dark space during the eclipsed portion of each orbit. The dark signal is fitted to four instrument temperatures to model the contributions from different portions of the instrument. The instrument temperatures during solar measurements are used to estimate the background contribution to the solar signal at actual observing times.

The dark signal data numbers are converted to irradiances using the TIM measurement equation without applying Doppler, solar distance, or pointing corrections, as these have no relevance for instrument thermal background. These dark irradiances are fitted to four instrument temperatures, which form the basis vectors for modeling the observed dark irradiances with the linear combination

$$D_{\text{Dark}} \approx \sum_{J=1}^{4} C_J T_J^4, \tag{3}$$

where the C_J are determined for best fit and T_J are the four Kelvin temperatures of the cavity, aperture plate, pre-baffle, and shutter. Since the basis vectors in Equation (3) are highly correlated, the Singular Value Decomposition (SVD) method of Press *et al.* (1993) is used to isolate individual temperature dependences of the dark signal. The coefficients C_J from the SVD fit have little physical significance and vary sufficiently that the SVD fit is computed daily using a 7-day running fit to background measurements, rather than presuming the C_J remain constant with time. The thermal background during the actual solar observations is then estimated by applying this temperature dependence to the daytime portion of the orbit and using actual instrument temperatures measured during the solar observations.

Dark signals of roughly $-3.15\,\text{W/m}^2$ are measured. (The negative value is due to the *loss* of energy from the cavities into space when the shutter is opened, so the dark correction increases the measured TSI.) This value varies due to thermal fluctuations in the instrument by $0.1–0.2\,\text{W/m}^2$ between orbit sunset and sunrise,

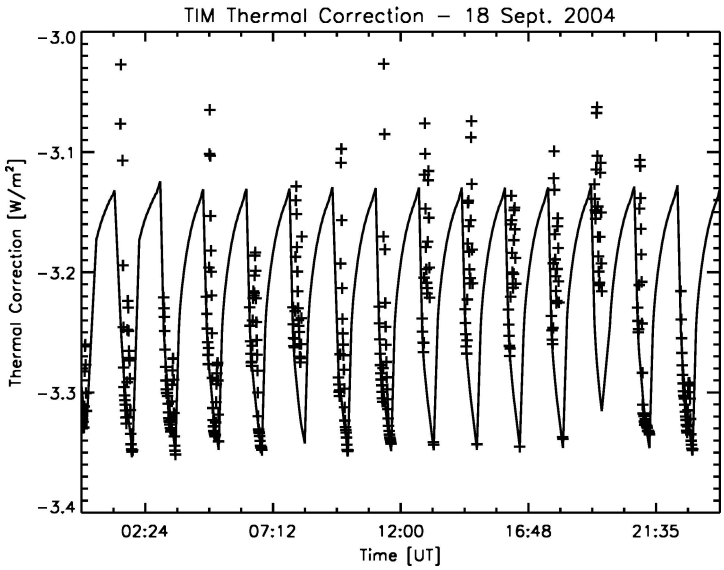

Figure 8. Dark signal observations and model. A fit of measured instrument temperatures to measured signals of dark space ('+' *signs*) gives a model of the thermal contributions of the instrument signal. This model estimates the thermal contribution at the temperatures relevant during solar observations (*solid line*).

as shown in Figure 8, giving a relative effect during the orbit of ∼100 ppm. The uncertainty on this dark correction is approximately 0.01 W/m^2, or less than 10 ppm of the solar signal.

3.2. SERVO LOOP GAIN IS MONITORED ON ORBIT BY ANALYZING THE RESPONSE TO A STEP FUNCTION INPUT

The primary ESR is thermally balanced against a reference ESR maintained at constant temperature by an AC bridge circuit operated at 100 Hz. A DSP maintains the ESR thermal balance by applying heater power to the primary cavity. The gain of this servo loop at the 0.01 Hz shutter fundamental affects the measured signal when responding to non-equilibrium conditions. The DSP prevents such conditions by applying a feedforward signal to the ESR anticipating power changes as the shutter transitions between open and closed.

The servo gain is calibrated by the DSP monthly to a relative accuracy of 4.5×10^{-4} (see Figure 9). We further set the feedforward value within 1% of the anticipated ESR power level after a shutter transition, reducing the sensitivity of the TSI measurement to uncertainty in gain. For TIM gains, with the real part of $G \approx 60$, the gain dependent term is thus a $<10^{-3}$ relative correction causing relative uncertainty in the final TSI ∼ 0.1 ppm.

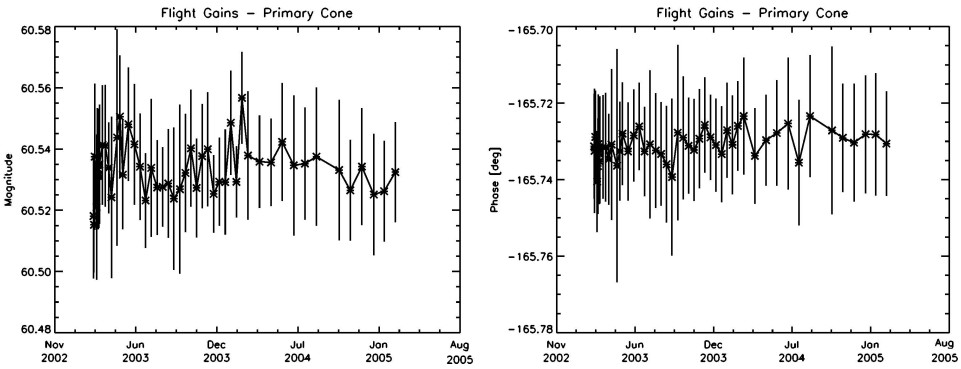

Figure 9. On-orbit servo gain calibrations. Gain of the primary cavity is measured at least monthly by analyzing the response to a DSP-provided step function. Both gain magnitude (*left*) and phase (*right*) are very constant with time. Note the small vertical scales on the plots. Uncertainties are indicated by *vertical bars*.

3.3. DEGRADATION IS MONITORED VIA DUTY CYCLING ESRS AND REFLECTANCE-TRACKING PHOTODIODES

Simultaneous, pair-wise inter-comparisons of the four cavities used to measure TSI allows monitoring for long-term changes in cavity absorption, with the exposure-dependent degradation expected to be lower in the lesser-used cavities. A photodiode monitors the light reflected from each cavity, and has gain set such that it is very sensitive to small changes in cavity reflectance. A ground program to monitor unused witness ESR cavities tracks reflectance changes of the cavity due to time alone.

The primary ESR is compared against the other, lesser-used ESRs regularly. Measurements with the primary ESR are acquired nearly continually. Simultaneous measurements of the Sun with both the primary and secondary ESR are done 1% of the time, or for one SORCE orbit per week. The secondary and tertiary ESRs acquire simultaneous measurements 0.5% of the time, and the fourth ESR is used simultaneously with the primary 0.2% of the time. Exposure effects can thus be tracked and corrected by a degradation factor that starts at unity at launch.

The primary ESR shows a slight decrease in its sensitivity that is likely due to an increase over the first 2 years of on-orbit operations in the cavity reflectance by $<$90 ppm (see Figure 10). This increase is due to solar brightening of the nickel phosphorus (NiP) black cavity interiors. Compared to the traditional space-borne TSI-monitoring instruments (Fröhlich *et al.,* 1997; Willson and Hudson, 1991), this is a very small change of only 0.11 ppm/day and indicates the TIM's NiP black cavity interior (described by Kopp and Lawrence, 2005) is more robust than the black paints used in other instruments. These sensitivity changes in the TIM are tracked to $<$10 ppm/year.

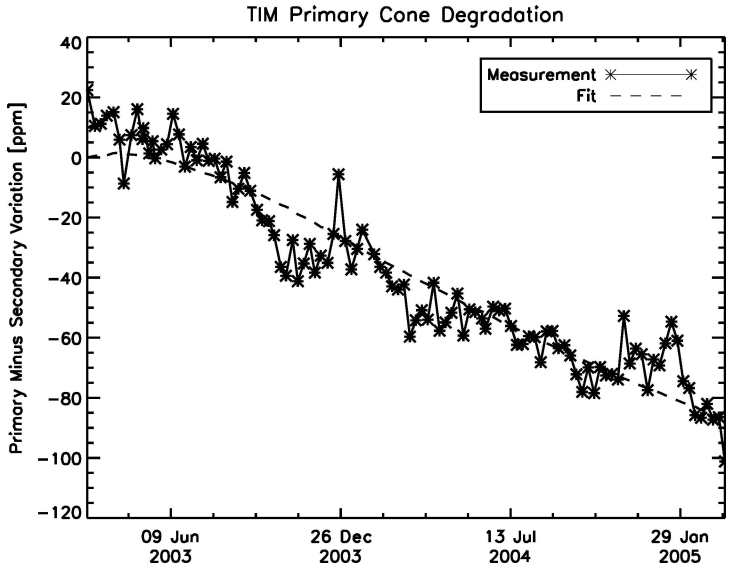

Figure 10. ESR degradation. The primary ESR is 87 ppm less sensitive than just after launch due to solar exposure related degradation through March 2005. A fit (*dashed*), based on photodiode signals, smoothes the measurements (*asterisks*).

Through March 2005, the four TIM ESRs acquired 235, 3.9, 0.98, and 0.47 days of cumulative solar exposure. At the degradation rate observed for the primary ESR and the current duty cycling rates, the other ESRs will not show any signs of solar exposure dependent degradation by the end of the SORCE's 5-year mission.

The photodiodes monitoring the reflection from each of the four cavities show results consistent with the inter-cavity comparisons. All photodiodes show similar radiation damage (independent of solar exposure) that lowers their sensitivity. After correction for this nearly exponential decrease in sensitivity, the photodiodes indicate no changes in the lesser-used ESRs, and a ∼72 ppm increase in reflectance of the primary ESR cavity (see Figure 11). The off-axis view angle of the photodiodes into the cavities and/or the different spectral responses of the photodiodes from the ESRs likely account for the difference between the 72 ppm photodiode-determined increase in the primary ESR reflectance and that determined by the inter-cavity comparisons; the photodiode signals are useful mainly for indicating relative cavity reflectance changes.

3.4. SPACECRAFT POSITION IS KNOWN TO HIGH ACCURACY

Spacecraft position and velocity knowledge correct measured irradiances to a constant solar distance of 1 AU. The measured irradiance varies inversely as the square

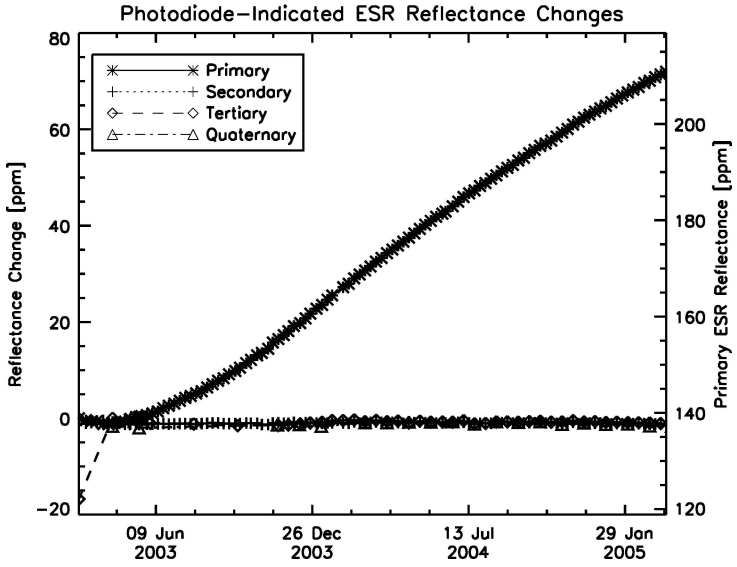

Figure 11. Photodiode signals. The TIM photodiodes monitoring ESR cavity reflectances show similar changes to the ESR comparisons, namely a brightening of the primary ESR interior with solar exposure. The primary ESR's reflectance, as indicated by the photodiode changes, is shown on the right-hand vertical axis. The three lesser-used cavities show almost no change in ESR brightness with time after correction for nearly equal radiation-induced changes in the photodiode sensitivity. The tertiary cavity has an errant initial measurement.

of the distance D (in AU) between the instrument and the Sun and directly with the radial velocity v toward the Sun. The distance and velocity corrections relate the measured value I_{meas} to that reported at a constant 1 AU by

$$I_{1\text{AU}} = \frac{I_{\text{meas}}}{(1 + 2v/c)1/D^2}, \tag{4}$$

where c is the speed of light. The factor of 2 in the velocity correction includes the effects of both a Doppler shift and a change in photon collection rate.

Contributions to the Sun-to-spacecraft distance and velocity come from the spacecraft's orbit around the Earth and the Earth's orbit around the Sun. These are precisely known from North American Aerospace Defense Command (NORAD) tracking data and NASA/JPL ephemerides respectively.

SORCE data processing involving the Earth–Sun distance and velocity uses the JPL VSOP87 ephemeris described by Bretagnon and Francou (1988). The VSOP87D solution, which gives heliocentric positions in spherical coordinates reckoned to the mean ecliptic and equinox for any desired date, is applied. The computed ephemeris positions agree with those in the *Astronomical Almanac* to ± 1 in the least significant digit tabulated.

TABLE I
JPL ephemeris and NORAD uncertainties.

	σD (km)	σv (m s^{-1})
JPL ephemeris VSOP87	3.7	0.04
NORAD TLE/SGP4	0.5	1.0
Total (RSS)	3.7	1.0

Knowledge of the spacecraft's position and velocity relative to the Earth are derived from propagations of the NORAD two-line-element (TLE) sets using the SGP4 propagation model. These TLEs, used to track thousands of Earth-orbiting objects, are reported regularly courtesy of NORAD. At an orbit of 640 km, the SORCE spacecraft's orbital parameters are fairly stable.

Using the full VSOP87 precision and NORAD TLE updates about every 18 h, the approximate distance and velocity uncertainties from both are shown in Table I. The JPL ephemeris is the dominant source of uncertainty in the spacecraft's distance to the Sun, and NORAD is the dominant uncertainty in radial velocity, although neither is significant; position and velocity uncertainties contribute to TIM accuracy uncertainties by less than 0.05 and 0.01 ppm respectively.

3.5. Sensitivity to pointing is low

Although several FOV maps have been done on-orbit for the benefit of other SORCE instruments, these pointing characterizations are not sensitive at the $<$50 ppm level needed to discern TIM pointing sensitivity from normal TSI fluctuations caused by solar oscillations. This is not unexpected, since the pre-launch analysis described in Section 2.6 indicated little sensitivity to pointing. Currently, no pointing correction is applied to the TIM data.

4. Relative Standard Uncertainties as Flown

Table II summarizes post-launch estimates of the combined standard uncertainty, σ. These estimates include the ground-based calibrations of several instrument components and the on-orbit calibrations of others, and are assembled from calibrations at CU/LASP and/or NIST or from analyses. The dominant uncertainty is the knowledge of non-linearity in the power applied to the flight ESRs, as these are only measured using ground-based TIM instruments and are adjusted to be consistent with flight-unit test measurements.

The quadrature sum of the flight uncertainties gives a total standard uncertainty slightly in excess of 200 ppm.

TABLE II

TIM uncertainty budget summary as flown (uncertainties are 1 standard deviation).

Factors/corrections	Size (ppm)	σ (ppm)
Distance, f_{AU}	33 537	0.1
Velocity, f_{Dopp}	57	0.7
Shutter waveform, S	100	1
Aperture, A	1 000 000	55
Reflectance, $1 - \alpha$	200	54
Servo gain, G	16 000	0
Standard, V^2	1 000 000	7
Non-linearity	1000	∼186
Standard, R	1 000 000	17
Equivalence, $\mathbf{Z}_H/\mathbf{Z}_R$	7	22
Dark signal	2700	10
Scattered light	100	25
Repeatability (noise)		1.5
Total (RSS)		∼205

5. Summary

The ground- and flight-based TIM calibrations are much as designed with the exception of the non-linearity in applied power. This has been corrected using precise measurements of two ground-based TIM units, although it limits the combined standard uncertainty of the TIM to ∼205 ppm.

Comparisons of the TIM to other TSI radiometers are described by Kopp, Lawrence, and Rottman (2005).

Acknowledgements

This research was supported by NASA contract NAS5-97045. Generous contributions from NIST enabled the small uncertainties achieved. LASP engineers and managers are to credit for the instrument assembly and calibration facilities.

References

Bretagnon, P. and Francou, G.: 1988, *Astron. Astrophys.* **202**, 309.

Fowler, J., Saunders, R., and Parr, A.: 2000, *Metrologia* **37**, 621.

Hanssen, L. M., Khromchenko, V., Prokhorov, A., and Mekhontsev, S.: 2003, in *Proceedings of the 2003 CALCON Program*, Logan, UT.

Fröhlich, C., Crommelynck, D. A., Wehrli, C., Anklin, M., Dewitte, S., Fichot, A., Finsterle, W., Jimenez, A., Chevalier, A., and Roth, H.: 1997, *Solar Phys.* **175**, 267.
Kopp, G. and Lawrence, G.: 2005, *Solar Phys*., this volume.
Kopp, G., Lawrence, G., and Rottman, G.: 2005, *Solar Phys*., this volume.
Lawrence, G. M., Rottman, G., Harder, J., and Wood, T.: 2000, *Metrologia* **37**, 407.
Lean, J.: 2000, *Geophys. Res. Lett.* **27**, 16.
Press, W., Teutolsky, S., Vetterling, W., and Flannery, B.: 1993, *Numerical Recipes: The Art of Scientific Computing*, Cambridge University Press, Cambridge.
Shirley, E.: 1998, *Appl. Opt.* **37**, 28, 6581.
Shirley, E.: 2000, *NIST Report of Modeling 0000207602*.
Spreadbury, P. J.: 1991, *IEEE Trans. Instrum. Meas.* **40**, 343.
Willson, R. C. and Hudson, H.: 1991, *Nature* **351**, 42.